IN-34
198131
11P

NASA Technical Memorandum 106427
AIAA-93-1966

Pressurization and Expulsion of a Flightweight Liquid Hydrogen Tank

N.T. Van Dresar and R.J. Stochl
Lewis Research Center
Cleveland, Ohio

(NASA-TM-106427) PRESSURIZATION AND EXPULSION OF A FLIGHTWEIGHT LIQUID HYDROGEN TANK (NASA) 11 p

N94-20177

Unclas

G3/34 0198131

Prepared for the
29th Joint Propulsion Conference and Exhibit
cosponsored by the AIAA, SAE, ASME, and ASEE
Monterey, California, June 28–30, 1993

NASA

PRESSURIZATION AND EXPULSION OF A FLIGHTWEIGHT LIQUID HYDROGEN TANK

N. T. Van Dresar*
and
R. J. Stochl

National Aeronautics and Space Administration
Lewis Research Center
Cleveland, Ohio 44135

Abstract

Experimental results are presented for pressurization and expulsion of a flightweight 4.89 m^3 liquid hydrogen storage tank under normal gravity conditions. Pressurization and expulsion times were parametrically varied to study the effects of longer transfer times expected in future space flight applications. It was found that the increase in pressurant consumption with increased operational time is significant at shorter pressurization or expulsion durations and diminishes as the duration lengthens. Gas-to-wall heat transfer in the ullage was the dominant mode of energy exchange, with more than 50 percent of the pressurant energy being lost to tank wall heating in expulsions and the long duration pressurizations. Advanced data analysis will require a multidimensional approach combined with improved measurement capabilities of liquid-vapor interfacial transport phenomena.

Nomenclature

A area
c specific heat
E total energy
h specific enthalpy
M total mass
m mass
$\dot{m}$ flowrate, mass transfer rate
P pressure
Q total heat leak
$\dot{q}$ heat flux
R gas constant for hydrogen
T temperature
$\overline{T}$ average temperature
t time
U total internal energy
u specific internal energy
V volume
x mass fraction
Z compressibility factor
ρ density

subscripts
e interfacial transport (+ for evaporation)
i summation index
id ideal
im initial mass in vapor region
in entering tank
nh normal-hydrogen
ℓ liquid
o outflow
p pressurant
ph parahydrogen
v vapor
w wall
1 start
2 end

Introduction

Future NASA missions will involve pressurization and expulsion of cryogenic tankage on-orbit or in other low-gravity environments. Understanding of low-gravity effects such as the undetermined liquid-vapor phase distribution and its impact on tank pressurization and expulsion will require space experimentation and vastly improved computational modeling capabilities of low gravity fluid dynamics and interfacial heat/mass transport. A related issue pertaining to cryogen transfer operations is the influence of longer duration pressurization and expulsion processes due to various operational constraints involved with low-gravity cryogenic fluid management. Longer operational times are expected due to requirements imposed by unvented transfer processes and liquid acquisition devices. Reference 1 provides a summary of pressurization technology and low-gravity issues.

This paper partially addresses the issue of longer pressurization and expulsion times by examining the effects occurring in the normal gravity environment. Experiments were conducted in a flightweight liquid hydrogen (LH_2) tank representative of future spacecraft tankage. This tank had a low mass-to-volume ratio and high performance multilayer thermal insulation. Pressurization tests from atmospheric pressure to 205 or 275

*member, AIAA

Copyright © 1993 by the American Institute of Aeronautics and Astronautics, Inc. No copyright is asserted in the United States under Title 17, U.S. Code. The government has a royalty-free license to exercise all rights under the copyright claimed herein for Governmental purposes. All other rights are reserved by the copyright owner.

kPa were performed at nominal fill levels of 50 and 87 percent (by volume). Expulsion tests were performed from 87 to 5 percent fill at constant tank pressures of 205 and 275 kPa. The main objectives of the tests were to determine the influence of ramp and expulsion times on the required pressurant mass. Ramp times (times to pressurize the tank to the expulsion pressure) were parametrically varied from 0.23 to 8.2 min; the range of expulsion time was from 12 to 33 min. Ambient temperature hydrogen gas was used as the pressurant.

Similar LH_2 tests were conducted in thicker-walled spherical tanks more than two decades ago[2,3]. Results of these studies indicated that inlet gas temperature, tank pressure level and injector geometry had the greatest impact on pressurant requirements. Tank wall thickness (0.41-0.89 cm compared to 0.21 cm for the present work) was reported to have a lesser influence. Ramp durations for the present work are up to 9 times those of the earlier work and expulsions are up to 75 percent longer. The present data is analyzed in a similar manner and compared to the earlier results[2,3].

Apparatus

Tests were conducted in a vacuum chamber with a cryoshroud enclosing the LH_2 test tank and a smaller companion tank (unused for these tests). The shroud was kept at ambient temperature (295 K) thus maintaining a constant heat flux to the test article. Vacuum chamber pressures were on the order of 10^{-4} to 10^{-3} Pa. The LH_2 test tank is constructed of chemical-milled 2219 aluminum and insulated with multi-layer insulation. It is approximately an ellipsoidal volume of revolution having a major-to-minor axis ratio of 1.2, a major diameter of 2.2 m, a volume of 4.89 m^3, and an internal surface area of 14.0 m^2. A 0.71 m diameter flange at the top provides access to the inside. The tank mass is 149 kg. Most of the wall is 2.08 mm thick except for the thick bolted flange and lid at the top, thickened lands for support lugs, and a thickened equatorial region. The tank insulation system, size, and lightweight construction (except for the lid) are representative of the type of system that may be used in future space transfer vehicles.

Pressurant gas from outside high pressure storage bottles entered the tank through a conical diffuser at the top. The diffuser outlet was 15.2 cm in diameter and is about 12 cm below the tank lid. Two wire cloth screens were positioned within the diffuser for flow smoothing. A silicon diode transducer mounted inside the diffuser measured incoming gas temperature. Pressurant gas flow rate was measured at a sharp-edged orifice equipped with high and low range differential pressure transducers. Liquid outflow exited at the tank bottom and was measured by a venturi meter in the transfer line.

Tank pressure was measured by pressure transducers located in the vent line. Liquid level was measured by a capacitance probe. Fluid temperatures were measured in both the vertical and radial directions by an array of silicon diode transducers as shown in Fig. 1. Four radial temperature rakes were suspended from the main vertical rake as shown. Two interface rakes having sensors spaced at 0.64 cm intervals were employed to obtained detailed measurements near the liquid-vapor interface at the 50 and 87 percent fill locations. The external wall temperature distribution was measured by a number of wall-mounted silicon diode transducers as indicated in Fig. 1. Open symbols in Fig. 1 denote failed sensors not used in the data analysis. Boil-off tests were not conducted during the current tests—on the basis of other test results using the same hardware, the average wall heat flux is estimated to be 2.3 W/m^2.

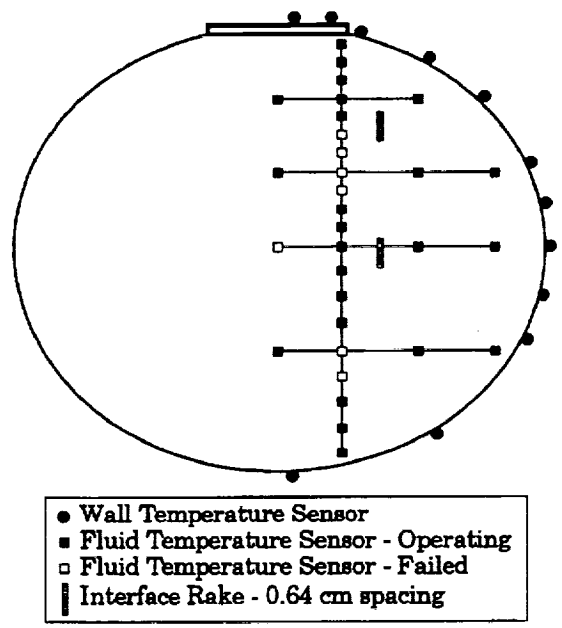

Figure 1 - Schematic of Test Tank Showing Temperature Sensor Locations.

Test Procedures

The tank was filled to the starting fill level while the tank pressure was kept above atmospheric pressure and then vented to atmosphere to induce bulk liquid boiling and isothermal liquid conditions. The tank remained vented for at least 15 min until saturated conditions at atmospheric pressure were established. A ramp test was

initiated by closing the vent valve and opening the pressurant line valves. A preset pressure ramp rate was maintained by an automatic ramp generator connected to the flow control valve. Ramp tests were stopped when the final tank operating pressure was reached. For expulsions, control of the pressurant flow valve was switched to an automatic pressure controller which added pressurant to maintain constant tank pressure. Liquid outflow was regulated by remote operation of flow control valves in the outflow line. Expulsions were terminated when the liquid fill level dropped below 5 percent. Data was sampled and recorded at regular intervals by an automated data acquisition system. Ranges of ramp and expulsion times were determined by limitations of the maximum gas supply rate and the lower limit of flow rate measurement capabilities at the test facility.

Data Analysis

The pressurant flowrate (from the gas orifice equation) was integrated over the test duration to obtain the total pressurant mass added in each test.

$$M_p = \int \dot{m}_p dt \tag{1}$$

Pressurant collapse factors are defined as the ratio of actual pressurant requirements to an ideal amount. The ideal gas requirement for ramp pressurization was calculated as

$$M_{p,id} = \frac{P_2\left(V_{im,1} - V_{im,2}\right)}{Z_2 R \overline{T}_p} \tag{2}$$

where $V_{im,2}$ is the volume of the initial ullage mass after isentropic compression from P_1 to P_2. $V_{im,2}$ was obtained from hydrogen thermodynamic properties. For expulsion, the ideal mass is given by

$$M_{p,id} = \frac{P_2 \Delta V_v}{Z_2 R \overline{T}_p} \tag{3}$$

A compressibility factor of unity was calculated for all tests.

Transient vapor mass calculations assumed that uniform radial temperature distributions prevailed. Discussion of the validity of this assumption is deferred until later. Using the vapor temperature measurements along the main vertical temperature rake, plus other locations when necessary to substitute for failed sensors, a temperature profile for the vapor region was obtained at discrete times during a test. The temperature profiles were individually fitted with smooth interpolated curves. Temperatures were then obtained at regular vertical intervals over the range of the vapor space and used along with the instantaneous tank pressure to get local vapor properties from a fluid properties subroutine. The data analysis code determined the volumes for each vapor segment and integrated the density-volume relation to obtain total vapor mass at each time period.

$$M_v(t) = \int \rho_v dV_v \tag{4}$$

The rate of change of vapor mass versus time is equal to the instantaneous pressurant flowrate plus the mass transfer rate at the liquid-vapor interface (positive mass transfer defined as evaporation).

$$dM_v/dt = \dot{m}_p + \dot{m}_e \tag{5}$$

Energy added to the tank by the pressurant gas was obtained by integration of the product of flowrate and specific enthalpy.

$$E_p = \int_1^2 \dot{m}_p h_p dt \tag{6}$$

A second, much smaller, tank energy addition term results from wall heat leak.

$$Q_{in} = \int \dot{q}_w A_w dt \tag{7}$$

Total wall energy change was determined from an analysis of wall temperature rise data.

$$\Delta U_w = \sum_i m_{w,i} c_{w,i} \Delta T_{w,i} \tag{8}$$

Total vapor energy at a given time was calculated using the specific internal energy.

$$U_v(t) = \int \rho_v u_v dV_v \tag{9}$$

Calculation of the change in vapor energy involved some uncertainty since the ullage was predominantly parahydrogen at the start of pressurization and then became a mixture as pressurant gas (normal hydrogen—75% ortho and 25% para) was added. Since the vapor composition was not known, it was assumed that the mass fractions of para and normal hydrogen were uniform throughout the ullage and thus determined from the following mass balance.

$$x_{ph,2} = \frac{x_{ph,1} M_{v,1} + M_e}{M_{v,2}}, \quad x_{nh,2} = \frac{x_{nh,1} M_{v,1} + M_p}{M_{v,2}} \tag{10}$$

All interfacial mass transfer was assumed to consist of parahydrogen only. Mass fractions calculated for the end of ramp tests were used as starting values for expulsions.

The change in total ullage energy relative to the initial state was calculated from the following:

$$\Delta U_v = \left(x_{ph}U_{v,ph} + x_{nh}U_{v,nh}\right)_2 - \left(x_{ph}U_{v,ph} + x_{nh}U_{v,nh}\right)_1 \quad (11)$$

The remaining term in an overall tank energy balance is the liquid energy increase, ΔU_ℓ, including that of the outflow, if any.

$$\Delta U_\ell = \left[\int \rho_\ell u_\ell dV_\ell\right]_2 - \left[\int \rho_\ell u_\ell dV_\ell\right]_1 - \int_1^2 \dot{m}_o h_o dt \quad (12)$$

Due to the extreme difference in liquid and vapor masses, very small temperature errors on the liquid-side will lead to large errors in the energy balance. To minimize this impact, liquid energy calculations for ramp tests were restricted to the region just below the liquid-vapor interface where a warm liquid layer develops due to heating from the vapor space. Thus, the energy change of the remaining liquid was assumed to be zero. All liquid was assumed to be parahydrogen. For expulsion tests, the entire liquid mass including outflow was included in the calculations. Two tests representing the extreme cases (high pressure/fast expulsion and low pressure/slow expulsion) were analyzed using 50 percent fill as the stopping point such that detailed temperature profiles in the warm liquid surface layer were available. Complete energy balance errors ranged from 1 to 6 percent—thus leading to confidence in the measurements and the one-dimensional analysis. Since there was no interface rake at the final expulsion liquid level of 5 percent fill, liquid energy increases for overall expulsions were calculated by subtracting the energy increase of the vapor and wall from the total energy input.

$$\Delta U_\ell = E_p + Q_{in} - \Delta U_v - \Delta Uw \quad (13)$$

Results

Table 1 provides the complete matrix of tests. The table gives operating parameters plus an indication of the radial temperature uniformity in the tank ullage. Tank pressure versus time histories were approximately linear for ramp tests. During expulsions, the tank pressure dropped suddenly by 5 to 20 kPa when the outflow valves were opened and then remained quasi-steady during expulsion with variations from 0 to +3 kPa. The final pressure is listed for expulsion tests. Pressurant temperatures listed are average values. Since the pressurant line was initially cold, the average gas temperature is slightly higher for tests of longer duration and higher total gas flow. Ullage temperatures were classified as radially uniform if radial variations did not exceed 2 percent of the maximum ullage gas temperature range. In tests where nonuniformities were

Table 1—Test Matrix

I.D.	Type	Operating Pressure [kPa]	Fill Level Range [%]	Test Duration [min]	Pressurant Temp [K]	Radial Temperature Uniformity
488	Ramp	102-207	87	0.233	271	No
487	Ramp	101-203	87	0.400	268	Yes
489	Ramp	101-205	87	0.950	272	Yes
490	Ramp	103-204	86	1.800	273	Yes
494	Ramp	100-278	86	0.400	284	No
493	Ramp	102-278	87	0.650	284	Approx.
492	Ramp	102-277	87	1.533	282	Yes
491	Ramp	101-275	87	3.000	280	Yes
498	Ramp	100-203	50	1.017	290	No*
497	Ramp	100-203	50	1.933	289	No
505	Ramp	101-203	49	4.900	291	Yes
499	Ramp	99-272	50	1.633	292	No*
500	Ramp	100-276	50	3.133	292	No
501	Ramp	102-276	49	8.217	291	Yes
506	Expulsion	201	87-5	12.667	294	Approx.
507	Expulsion	204	87-5	18.100	294	Yes
508	Expulsion	202	87-5	32.900	294	Yes
510	Expulsion	275	86-5	12.350	294	Approx.
509	Expulsion	277	86-4	18.150	295	Yes
511	Expulsion	279	87-5	32.967	292	Yes

observed, the variations occurred along the top radial temperature rake, with the higher temperature being at the position closest to the pressurant diffuser outlet. In some cases the departure from uniformity is considered small and restricted to the lowest density region of the ullage; these cases are denoted as having "approximate" uniformity. Two of the ramp tests at 50 percent fill showed extreme nonuniformity with radial variations observed along both radial temperature rakes in the ullage space—these tests are denoted with an asterisk. As expected, the nonuniformity is encountered at higher pressurant gas flowrates (jet-like flow at the diffuser outlet) occurring in quicker ramp processes, higher operating pressure and lower fill level (i.e., larger ullage volume to pressurize).

Figure 2 shows the total pressurant consumption for the pressurization process as a function of the ramp duration. As expected, the longer the ramp time, the more pressurant gas required. Also observed are the increasing pressurant requirements as the final tank pressure increases and as the tank liquid fill level decreases (increasing ullage volume). While this difference in actual pressurant mass for ramps may be small in comparison to pressurant needs for expulsions, it could become substantial in missions requiring

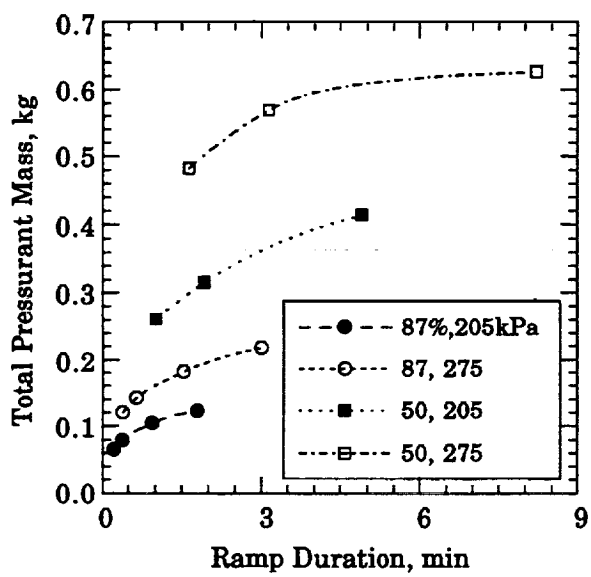

Figure 2 - Effect of Ramp Duration on Total Required Pressurant Mass.

multiple pressurizations of the supply tank. Collapse factors for the ramp tests are shown in Fig. 3. As expected, the faster ramps are more efficient—with collapse factors approaching 1.5. Some of the longer ramp times led to collapse factors greater than 3. At both fill levels, the ramps to higher final pressure show lower collapse factors for a given ramp time—thus indicating greater thermodynamic efficiency, albeit at higher pressurant mass requirements. Present results are thus consistent with earlier results[2,3] for trends with ramp time and fill level. Higher values for the present ramp collapse factors (1.6-3.2 vs. 1.1-1.8 for comparable fill levels) are due to the higher inlet gas temperature and lower final pressure in the present work. A trend also observed in the earlier work is the higher collapse factors at smaller ullage volume (larger fill level). This result was attributed to the colder average initial wall temperature at higher fill level which creates a larger temperature difference and higher rates of gas-to-wall heat transfer. Other factors are the higher wall surface-to-vapor volume ratio at 87 percent fill and the proximity of the diffuser to the liquid surface. The greater efficiency of the higher operating pressure indicates a lower fraction of pressurant energy is lost from the ullage space—this fraction is lower primarily because more pressurant energy is supplied to the ullage at the higher operating pressure and does not indicate reduced energy transfer. There is an increase in the sensitivities of required pressurant mass and collapse factor to time with decreasing time; performance benefits or penalties will be most significant when ramp duration is brief.

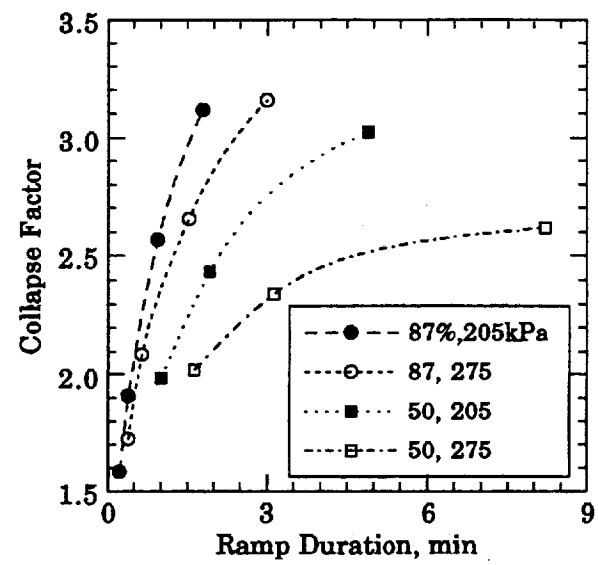

Figure 3 - Collapse Factors for Ramp Pressurization Experiments.

The effect of expulsion time on total pressurant consumption is shown in Fig. 4. Again, the amount of pressurant gas required during the expulsion period increases with increasing tank pressure. The increase in pressurant mass as the expulsion time increases becomes less at longer expulsion durations—at 205 kPa this trend is not apparent due to small variations in expulsion pressure.

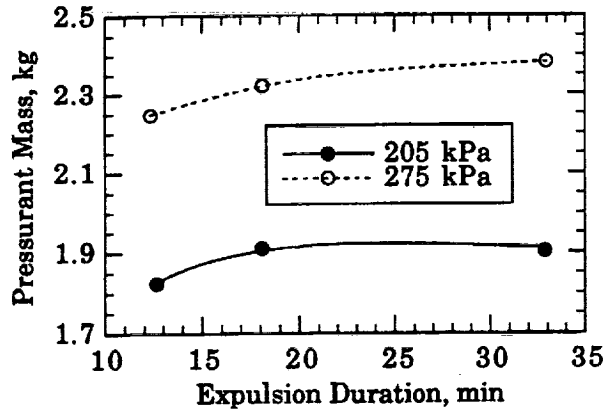

Figure 4 - Effect of Expulsion Duration on Total Required Pressurant Mass.

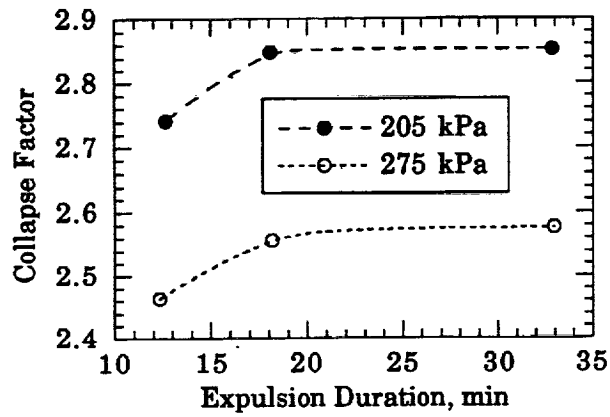

Figure 5 - Collapse Factors for Expulsion Experiments.

Collapse Factors for the expulsion tests are shown in Fig. 5. Trends are similar to the ramp results with collapse factor increasing with expulsion duration and decreasing with increasing expulsion pressure. Figs. 4 and 5 show that expulsion time has greatly reduced impact on pressurant requirements after a sufficiently long expulsion duration as been reached—approximately 18-20 min for these tests. These results indicate that beyond some characteristic time the required pressurant mass is less dependent upon expulsion time and that energy transfer from the vapor space occurs at a reduced rate. Figure 5 indicates a dependence of collapse factor on pressure level. This trend of decreasing collapse factor with increasing pressure is consistent with the above results for ramp pressurization. Results of ref. 3 did not exhibit this trend with pressure. Values of the present collapse factors (2.4-2.9) are comparable to earlier results[2,3] (2.3-3.3)—direct comparisons are difficult because of variations in pressurant gas temperature and expulsion pressure. It also appears that collapse factors are larger in smaller volume tanks; the ullage surface-to-volume ratio could be an additional controlling parameter.

Calculated interfacial mass transfer quantities are not reliable for ramp tests with radial vapor temperature nonuniformities. Remaining tests do not show conclusive results, other than that interfacial mass transfer is at most about 20 percent of the pressurant mass and could be either evaporation or condensation. Condensation was the more prevalent mode at 87 percent fill, possibly due to the close proximity of the diffuser outlet to the liquid-vapor interface. Mass and energy balance results are documented in Table 2.

The present energy balance calculations are also unreliable when radial temperature gradients exist. For some ramp tests with radially uniform vapor conditions, it was found that the calculated energy increase in the tank system still greatly exceeded the energy input. This result only occurred with the 87 percent fill tests and it is hypothesized that radial temperature variations also existed in the warm liquid layer near the interface. Only two ramp tests resulted in energy balance errors less than 10 percent—these were the tests at 50 percent fill with the longest ramp durations. For these tests, 49 percent of the incoming energy was lost to wall heating and 40-43 percent resulted in vapor energy increase. The liquid heating fraction was calculated to be from 8-15 percent. For ramp tests, the heat leak contribution to total energy input is small; from 0.2 to 0.7 percent of the total. Figure 6 shows the wall heating results—this data is considered valid for all ramp tests. Data for varying fill level and final ramp pressure appear to fall on a single curve with wall energy change going to zero as ramp duration approaches zero. As the time becomes large, the curve of wall energy fraction flattens considerably.

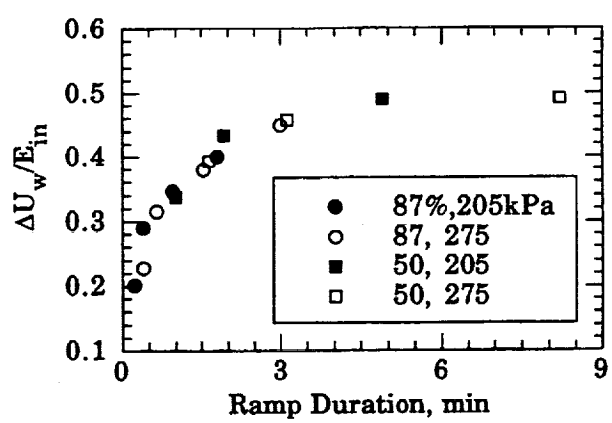

Figure 6 - Wall Energy Increase Fraction for Ramp Experiments.

Table 2—Mass and Energy Balance Results

I.D.	M_p [kg]	M_e[kg]	$x_{ph,2}$	E_p [kJ]	Q_{in} [kJ]	ΔE_v [kJ]	ΔE_w [kJ]	ΔE_ℓ [kJ]
488	0.0653	*0.006*	0.89	248	0.5	*159*	50	*194*
487	0.0793	0.001	0.87	299	0.8	164	87	*175*
489	0.1041	-0.013	0.82	398	1.8	177	138	*170*
490	0.1222	-0.025	0.80	469	3.5	181	189	*204*
494	0.1203	*-0.012*	0.78	481	0.8	*309*	109	*420*
493	0.1414	*-0.051*	0.74	565	1.3	*292*	178	*480*
492	0.1812	-0.027	0.71	719	3.0	309	274	*438*
491	0.2173	-0.027	0.66	856	5.8	315	387	*411*
498	0.2607	*0.016*	0.83	1062	2.0	*652*	360	256
497	0.3151	*-0.010*	0.80	1280	3.7	*653*	556	223
505	0.4141	-0.013	0.78	1695	9.5	676	836	152
499	0.4825	*0.000*	0.71	1983	3.2	*1105*	781	381
500	0.5685	*0.004*	0.66	2332	6.1	*1137*	1069	426
501	0.6255	0.101	0.66	2560	15.9	1117	1265	392
506	1.8244	0.294	0.30	7533	24.5	2312	4206	—
507	1.9114	0.275	0.29	7911	35.0	2356	4566	—
508	1.9029	0.505	0.33	7865	63.6	2324	4481	—
510	2.2480	0.307	0.24	9299	23.9	3063	4926	—
509	2.3218	0.406	0.25	9625	35.1	3091	5184	—
511	2.3823	0.581	0.29	9784	63.7	3102	5310	—

(Note: italicized results are most likely erroneous due to radial temperature gradients in vapor and/or liquid. Values are included for completeness only.)

Figure 7 provides the interfacial mass transfer fraction for the expulsion tests. The mode was evaporation in all cases and the amount of evaporated mass increases as a fraction of the pressurant requirement as the expulsion time increases. Although the fidelity of this data is marginal, the results demonstrate the significance of interfacial mass transfer in the expulsion process. The current results follow the trend of the earlier work[2,3] with increasing evaporation/ decreasing condensation as the expulsion duration becomes longer.

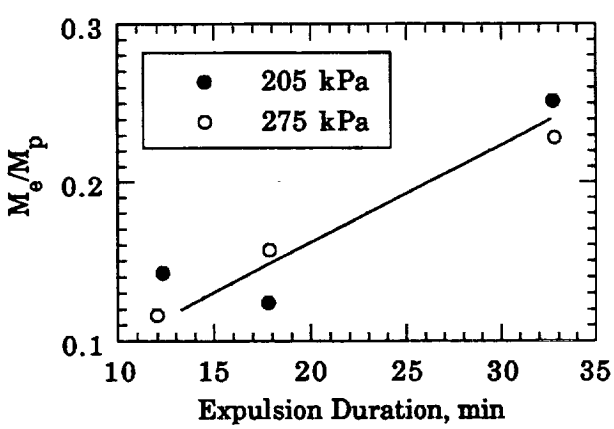

Figure 7 - Total Interfacial Mass Transfer for Expulsion Experiments.

Results of the energy balance analysis are shown in Fig. 8 for the expulsion tests. The distribution of energy input becomes independent of time after 18 min. At 275 kPa, about 53-54 percent of the energy added to the tank goes into wall heating, 32-33 percent remains in the ullage and the remainder, 14-15 percent, is lost to liquid heating. Results for the 205 kPa expulsions are similar, but with a slightly different distribution—56-57 percent goes into wall heating, 29-30 percent remains in the ullage and 13-14 percent lost to the liquid. For expulsions, the heat leak contribution to total energy input is from 0.3 to 0.8 percent of the total. The differing values for vapor heating fraction at the two pressures is the cause of the

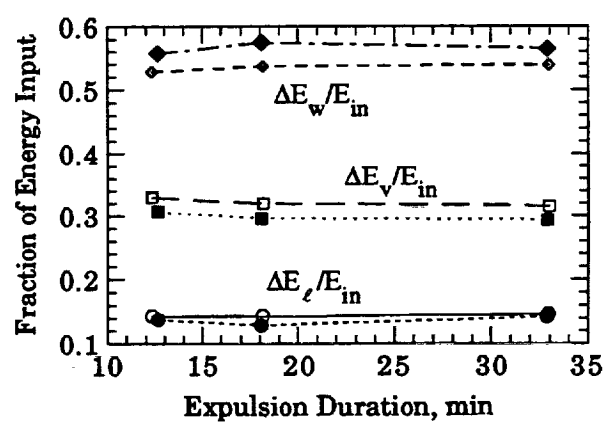

Figure 8 - Distribution of Tank Energy Input for Expulsion Tests (solid symbols-205 kPa, open-275 kPa).

collapse factor pressure dependence shown in Fig. 5. Earlier tests[2,3] show substantially reduced wall heating and increased vapor heating fractions as

the expulsion time decreases—the current data shows that the rate of change of the energy distribution fractions becomes small at longer expulsion times. Comparison of all data suggests that the characteristic time at which expulsion duration has little significance becomes greater as the tank size increases (decreasing tank surface-to-volume ratio).

Differences in the final temperature profiles at 5 percent fill for high pressure expulsions are evident in Fig. 9. There is an overall increase in end-of-expulsion vapor temperature as the expulsion duration decreases. Also shown is one of the initial temperature profiles at 87 percent fill—the starting profiles are essentially identical for other tests in the figure. The temperature profiles display the increased cooling of the ullage region as the expulsion duration increases—heat transfer is from the hotter vapor to the tank wall and liquid-vapor interface and results in an increase in the vapor density and mass. As the final temperatures decrease, the total energy change of the ullage increases due to the increased mass of the vapor. Similar final temperature profiles exhibiting vapor cooling with increasing process duration were observed for the low expulsion pressure and for ramp tests.

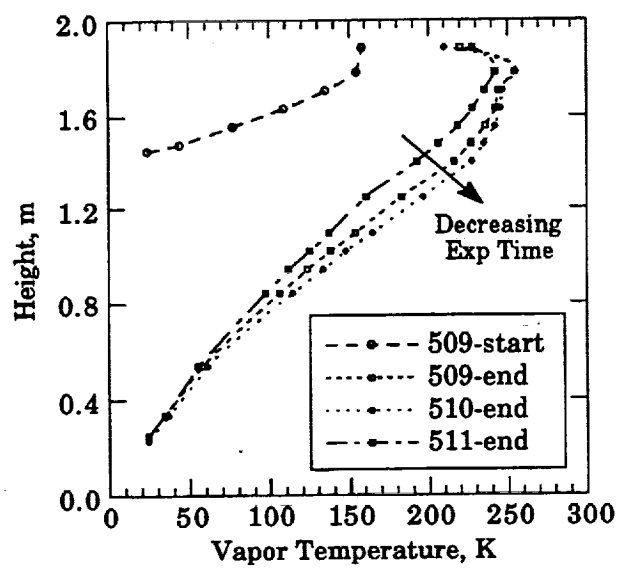

Figure 9 - Initial and Final Temperature Profiles for Expulsion Tests at 275 kPa

Vapor mass increase during the expulsion process is shown in Fig. 10 for the tests conducted at 275 kPa. Results for the 205 kPa tests are similar but not shown. Vapor mass increases linearly with time and the rate of increase decreases as the expulsion duration increases. The slope of these curves is the quantity dM_v/dt in Eq (5) and is approximately constant for each of the expulsion tests. Note that the final mass increases with increasing expulsion time—this result is due to the cooling of the vapor space that increases with time as discussed in connection with Fig. 9. Since the pressurant gas flow rate and dM_v/dt remain essentially constant during outflow, it follows from Eq. (5) that the interfacial mass transfer rate is also approximately constant. This occurs although the interfacial area and (presumably) warm liquid layer thickness are changing throughout the expulsion process.

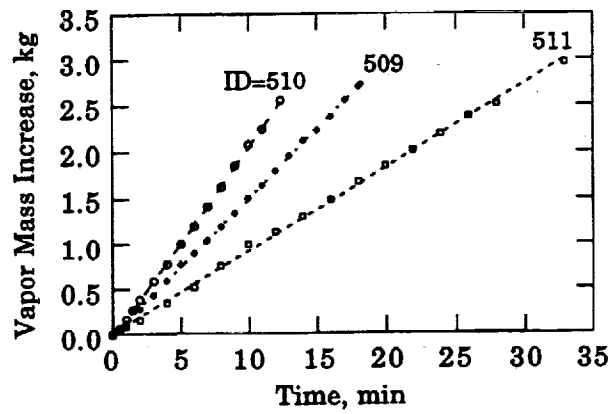

Figure 10 - Vapor Mass During Expulsion, 275 kPa.

The computed vapor mass increase during ramp tests to 275 kPa at 87% fill are shown in Fig. 11. The two longer duration tests (I.D. 491 and 492) exhibit smooth upward curving profiles. The fast ramp test (494) is shown for comparison and displays scattered data points which are attributed to the non-uniform radial temperatures observed in this test—therefore, the data shown for 494 should not be considered accurate. Note that the same trends occur here as for the expulsion tests. As the ramp duration increases, the final vapor mass increases and the slope of the curve becomes less. The curves with smooth profiles are well-represented by second order polynomial curve fits from which dM_v/dt is obtained. With dM_v/dt and the pressurant flow-rate known as functions of time, the transient interfacial mass transfer can be determined. Figure 12 shows the result for test 491. Unlike the expulsion tests, the mass transfer rate is not constant. The mass transfer is initially evaporation as expected since the tank is self-pressurizing when the pressurant flow begins. As the pressurant flowrate begins, the liquid becomes subcooled and the interface temperature increases—causing the evaporation rate to drop and the mass transfer mode switches to condensation as shown. For this particular case, the ramp duration is sufficiently long for the condensation rate to drop and the mass transfer

approaches the evaporation mode again. For shorter ramps, this approach to evaporation does not occur.

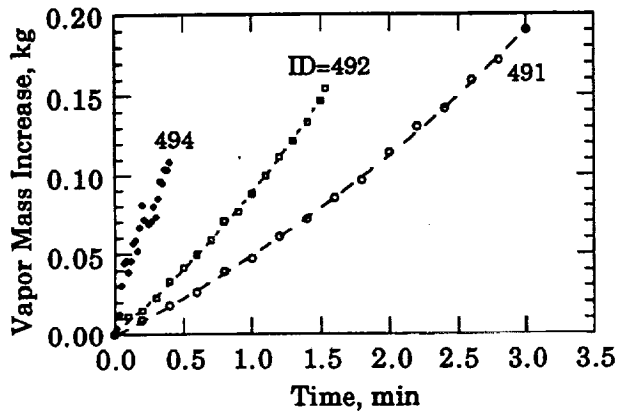

Figure 11 - Vapor Mass During Ramp, 87% Fill, 275 kPa Final Tank Pressure.

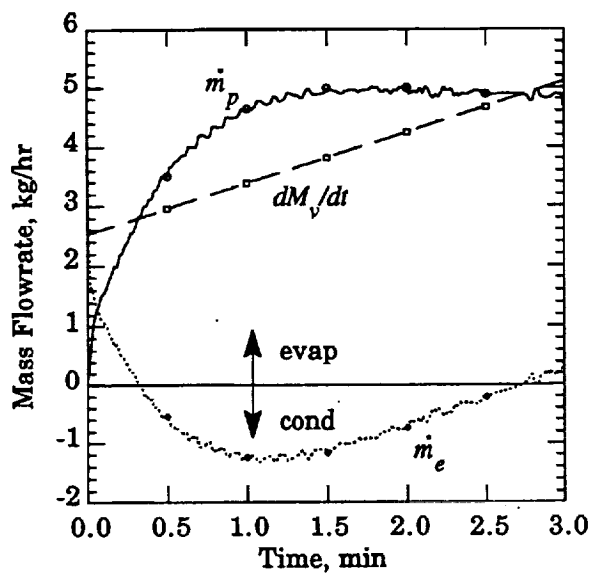

Figure 12 - Transient Vapor Mass Balance During Ramp Test I.D. 491, 87% Fill, 275 kPa Final Tank Pressure.

Conclusions

Pressurant gas requirements for both ramp and expulsion processes increase as the operational time is lengthened. For expulsions, it has been demonstrated that the rate of change of this increase becomes small at sufficiently long expulsion durations; based on observed trends, this effect also appears to hold for the ramp process. The diminishing rate of change is attributed to the decreased rate of energy transfer from the ullage gas due to decreasing temperature gradients near the tank wall and liquid surface as the process duration becomes long.

The present work combined with previous results gives reasonable indications of the quantitative dependence of the collapse factor on tank pressure, pressurant gas temperature, wall thickness and process duration for the normal gravity environment. With careful examination of collapse factor data and trends, one can use collapse factors to estimate pressurant gas requirements. Additional tests would be useful to extend the current range of collapse factor data where necessary.

In the present study, the distribution of pressurant energy to ullage, liquid and wall heating was insensitive to the process time as expulsions became long. The largest portion of input energy goes into wall heating—50 percent or more for expulsions and long ramps. It is hypothesized that for extremely long durations or tanks with less heat capacity, the wall heat capacity would be reached; at this point the liquid heating fraction would increase. In this situation, the wall thickness would have greater influence.

Interfacial mass transfer plays a significant role in ramp or expulsion processes of practical duration. Although accurate data remains difficult to obtain, it is recognized that dependable analytical tools will require proper modeling and improved measurement capabilities of interfacial transport phenomena.

It is clear that one-dimensional analysis is not always adequate for analysis of real systems. Radial gradients were sometimes observed in the vapor region and suspected in the liquid. This was apparent in ramp tests involving rapid pressurization and high liquid fill level. One-dimensional analysis of the expulsion process was found to be acceptable for the present work, but this approach should be treated with caution.

References

1. Van Dresar, N.T., "Pressurization of Cryogens: A Review of Current Technology and its Applicability to Low-Gravity Conditions," AIAA paper 92-3061, 1992.

2. Stochl, R.J., *et al*, "Gaseous-Hydrogen Requirements for the Discharge of Liquid Hydrogen From a 1.52 Meter- (5-ft-) Diameter Spherical Tank," NASA TN D-5336, 1969.

3. Stochl, R.J., *et al*, "Gaseous-Hydrogen Pressurant Requirements for the Discharge of Liquid Hydrogen From a 3.96 Meter- (13-ft-) Diameter Spherical Tank," NASA TN D-5387, 1969.

REPORT DOCUMENTATION PAGE

Form Approved
OMB No. 0704-0188

Public reporting burden for this collection of information is estimated to average 1 hour per response, including the time for reviewing instructions, searching existing data sources, gathering and maintaining the data needed, and completing and reviewing the collection of information. Send comments regarding this burden estimate or any other aspect of this collection of information, including suggestions for reducing this burden, to Washington Headquarters Services, Directorate for Information Operations and Reports, 1215 Jefferson Davis Highway, Suite 1204, Arlington, VA 22202-4302, and to the Office of Management and Budget, Paperwork Reduction Project (0704-0188), Washington, DC 20503.

1. AGENCY USE ONLY (*Leave blank*)

2. REPORT DATE
December 1993

3. REPORT TYPE AND DATES COVERED
Technical Memorandum

4. TITLE AND SUBTITLE
Pressurization and Expulsion of a Flightweight Liquid Hydrogen Tank

5. FUNDING NUMBERS
WU–506–42–73

6. AUTHOR(S)
N.T. Van Dresar and R.J. Stochl

7. PERFORMING ORGANIZATION NAME(S) AND ADDRESS(ES)
National Aeronautics and Space Administration
Lewis Research Center
Cleveland, Ohio 44135–3191

8. PERFORMING ORGANIZATION REPORT NUMBER
E–8269

9. SPONSORING/MONITORING AGENCY NAME(S) AND ADDRESS(ES)
National Aeronautics and Space Administration
Washington, D.C. 20546–0001

10. SPONSORING/MONITORING AGENCY REPORT NUMBER
NASA TM–106427
AIAA–93–1966

11. SUPPLEMENTARY NOTES
Prepared for the 29th Joint Propulsion Conference and Exhibit cosponsored by the AIAA, SAE, ASME, and ASEE, Monterey, California, June 28–30, 1993. Responsible person, R.J. Stochl, (216) 977–7522

12a. DISTRIBUTION/AVAILABILITY STATEMENT
Unclassified - Unlimited
Subject Category 34

12b. DISTRIBUTION CODE

13. ABSTRACT ***(Maximum 200 words)***

Experimental results are presented for pressurization and expulsion of a flightweight 4.89 m^3 liquid hydrogen storage tank under normal gravity conditions. Pressurization and expulsion times were parametrically varied to study the effects of longer transfer times expected in future space flight applications. It was found that the increase in pressurant consumption with increased operational time is significant at shorter pressurization or expulsion durations and diminishes as the duration lengthens. Gas-to-wall heat transfer in the ullage was the dominant mode of energy exchange, with more than 50 percent of the pressurant energy being lost to tank wall heating in expulsions and the long duration pressurizations. Advanced data analysis will require a multidimensional approach combined with improved measurement capabilities of liquid-vapor interfacial transport phenomena.

14. SUBJECT TERMS
Pressurization; Fluid transfer

15. NUMBER OF PAGES
11

16. PRICE CODE
A03

17. SECURITY CLASSIFICATION OF REPORT
Unclassified

18. SECURITY CLASSIFICATION OF THIS PAGE
Unclassified

19. SECURITY CLASSIFICATION OF ABSTRACT
Unclassified

20. LIMITATION OF ABSTRACT